Received: 10 April 2018 | Revised: 6 July 2018 | Accepted: 7 July 2018

DOI: 10.1111/jace.15940

ORIGINAL ARTICLE

Journal of the American Ceramic Society

Improvement of reliability and dielectric breakdown strength of Nb-doped lead zirconate titanate films via microstructure control of seed

Song Won Ko[1] | **Wanlin Zhu**[2] | **Charalampos Fragkiadakis**[1] | **Trent Borman**[2] | **Ke Wang**[2] | **Peter Mardilovich**[1] | **Susan Trolier-McKinstry**[2]

[1]Xaar plc, Cambridge, UK

[2]Materials Research Institute and Department of Materials Science and Engineering, The Pennsylvania State University, University Park, Pennsylvania

Correspondence: Song Won Ko, Xaar plc, 316 Science Park, Cambridge CB4 0XR, UK (songwon.ko@xaar.com).

Abstract

A $Pb(Zr,Ti)O_3$ (PZT) seed layer without Pb-deficient defective areas was developed to improve the dielectric breakdown strength and lifetime of thin film piezoelectric actuators. The proportion of defective area in the seed layers was reduced by adjusting the amount of Pb excess in the solution, combined with implementation of a dense, large-grained (>200 nm) Pt bottom electrode. The optimal Pb excess amount in the solution was about 20 at%; seeding was improved when a slightly Ti-rich composition (relative to the morphotropic phase boundary) was utilized. It was found that the dielectric breakdown strength and lifetime of PZT films improved as the proportion of visible defective area on the PZT seed layer decreased. Dielectric breakdown strength increased from approximately 300 kV/cm to about 1 MV/cm. The lifetime, characterized by highly accelerated lifetime testing, was increased 60 times by reducing the fraction of defective area. The activation energy (E_a) and voltage acceleration factor (N) for failure of devices (eg, patterned PZT films) were 1.12 ± 0.03 eV and 4.24 ± 0.07 respectively.

1 | INTRODUCTION

Lead zirconate titanate (PZT) thin films are utilized in a number of devices, including piezoelectric inkjet printheads and pyroelectric detectors.[1,2] The performance of these devices is enhanced when the orientation of the films produces the highest piezoelectric response. It is well-known that {001} textured PZT films near the morphotropic phase boundary (MPB) have the highest piezoelectric response.[3] The epitaxial growth method enables excellent {001} orientation,[4] but has not yet been scaled to large wafer sizes in a foundry environment for PZT films. Therefore, a seed layer of $PbTiO_3$, PbO, or $LaNiO_3$ is often deposited on the substrates before PZT deposition to obtain {001} texture.[5–8] However, these seed layers are not ideal due to the reduced piezoelectric properties caused by any residual $PbTiO_3$,[9] the potential for increased leakage current if the PbO content is not adequately controlled[10] and the high electrical resistivity of $LaNiO_3$.[11]

Recently Borman et al[12] reported improved orientation of an MPB PZT seed layer. This was achieved by optimizing the lead content in the solution and the PZT thicknesses for the template layer. Also, they found that the area fraction of defective material (visible pyrochlore phase) depends on the grain size of the bottom Pt electrode, with larger-grained Pt producing superior films. However, it is apparent from the microstructures that defective areas still remain for the pure PZT seed layers prepared from solutions with 10-16 at% excess lead content (ie, the entire range investigated). Therefore, this paper focuses on higher lead contents in the solution (up to 30 at%) with large-grained Pt bottom electrodes (>200 nm in grain size) in an

attempt to improve the seed layer microstructure. Nb-doped PZT (PNZT) films were investigated since Nb doping increases the dielectric, ferroelectric, and piezoelectric properties.[13] In addition, this paper investigates the relationship between the quality of the template layer, the dielectric breakdown strength, and the lifetime of the film under DC field. In this study the PNZT films were patterned; most of the data were taken on the wafer level and the highly accelerated lifetime testing (HALT) data was taken from devices fabricated using standard MEMS processing techniques.

2 | EXPERIMENTAL METHODS

Lead zirconate titanate seed layers with 2% niobium doping (PNZT) were made by spin-coating commercial 15 wt% PZT-E1 sol-gel solutions (Mitsubishi Materials Corporation, Tokyo, Japan) with varying lead excess (10-30 at%) on the platinized silicon substrate. Most of the solutions had a Zr:Ti ratio of 52:48, while one solution had a Zr:Ti ratio of 44:56, since Ti-rich PZT nucleates more readily in the perovskite phase.[14] Unlike Borman et al's[12] work, Pt with an average grain size of >200 nm was used (full width at half maximum of Pt {111} rocking curve ~1.5 ± 0.2°) for most of the samples, while the balance were prepared on Pt bottom electrodes with a grain size of ~25 nm. It was confirmed by transmission electron microscopy (TEM) that less Pb diffused into the Pt bottom electrode with the larger lateral grain size, due to the reduced number of grain boundaries (Figure S1). The solution was spin coated at 6000 rpm for 45 seconds, then pyrolyzed at 200°C for 2.5 minutes. Finally, the sample was crystallized in a rapid thermal annealer (RTA) at 700°C for 1 minute under two SLPM of O_2 flow with a heating rate of 10°C/s. The thickness of seed layer is around 55-60 nm.

After seed layer deposition, 15 wt% PNZT solutions with 16 at% Pb excess were spun on with 3000 rpm for 45 seconds and pyrolyzed at 100°C for 1 minute and 300°C for 4 minutes. The average Zr/Ti ratio was 52/48. The amorphous films were crystallized after every two spin-coated layers using the same thermal profile as the seed layer. The procedure was repeated until a thickness of ~1.9 μm was obtained (a total of 22 spin-coated layers).

The phase purity, crystallographic texture, and grain morphology were examined with X-ray diffraction (XRD, X'Pert Pro MPD; PANalytical, Almelo, The Netherlands) using Cu *K*α radiation and field-emission scanning electron microscopy (FE-SEM, Merlin; ZEISS, Oberkochen, Germany). The defective area fractions were quantified using ImageJ based on the FE-SEM images. TEM imaging and compositional analysis of the seed layer were conducted using a dual aberration corrected scanning/TEM (S/TEM) instrument operated at 200 kV (Titan; FEI Company, Hillsboro, OR, USA). The TEM specimens were prepared by an in situ milling and lift-out procedure in a focused ion beam (FIB, Helios NanoLab DualBeam 660; FEI Company). Before FIB milling, a protective carbon layer was electron beam deposited over the region of interest. After the specimen become electron transparent, the final cleaning was applied to both sample surfaces by using a 1 kV ion beam to remove the damaged layer produced during the FIB milling. Energy-dispersive spectrometry (EDS) maps were acquired across an area that included both perovskite PNZT and defective areas in the seed layer. Compositional mapping was performed using a SuperX EDS system which has four silicon drift detectors surrounding the sample, under scanning transmission electron microscopy (STEM) mode by using a high-angle annular dark field (HAADF) detector.

Dielectric breakdown strength was measured using an Aixacct DBLI tool (Aixacct Systems GmbH, Aachen, Germany) with 1 V steps and a 2-s hold time at each step (electrode area ~5×10^{-4} cm^2). HALT was used to determine the median lifetime of a population of PNZT capacitors at elevated temperatures and applied voltages. From these data the activation energy (E_a) and voltage acceleration factor (N) were calculated following the empirical equation from Prokopowicz and Vaskas.[15] Recently, a new model was proposed for voltage acceleration factor based on films where the leakage is controlled by the Schottky conduction mechanism,[16] but the microstructural inhomogeneity of the seed layer in this study precludes the use of that formalism. The devices were placed in a 24-pin DIP package and top electrodes were wire bonded to the contact pads of the package. HALT was performed using a Keithley picoammeter as a DC source and leakage current measurement tool.

3 | RESULTS AND DISCUSSION

It was found that the pyrolysis conditions are critical to achieve {100} orientation of the PZT seed layer. Borman et al used a two-step pyrolysis (100°C 1 minute + 300°C 4 minute) for deposition from a 12 wt% solution on finer grained Pt (25-80 nm). In this study, one-step and two-step pyrolysis procedures were explored. One-step pyrolysis was conducted in the 200-300°C temperature range; the two-step route added a 100°C drying step prior to the pyrolysis at temperatures of 200-300°C. However, with the 15 wt% solution on the larger grained Pt bottom electrodes, the optimized pyrolysis conditions producing {100} orientation were 200°C for 2.5 minutes, as shown in Figure 1.

Figure 2 shows microstructures of PNZT seed layers prepared from solutions with different excess lead contents. The arrows in Figure 2A-C mark examples of defective areas (which have the pyrochlore phase) in the PNZT seed. Defective areas were widespread, and occurred between

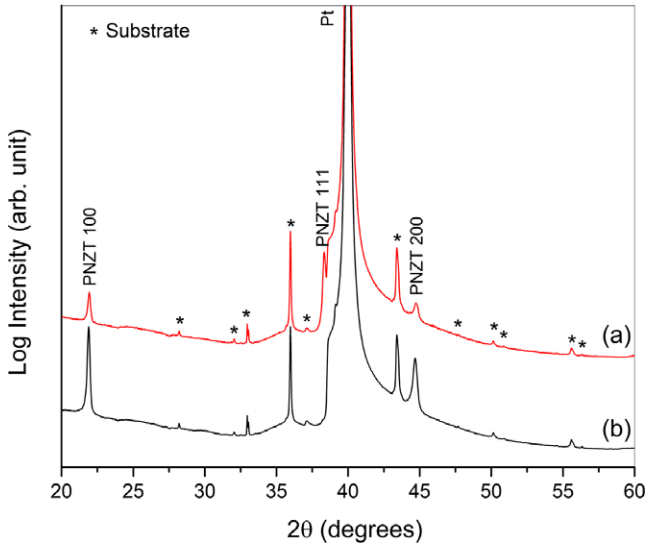

FIGURE 1 X-ray diffraction (XRD) patterns of Nb-doped PZT (PNZT) seed layers with 20 at% Pb excess in the solution; (a) 100°C + 300°C two-step pyrolysis and (b) 200°C one-step pyrolysis [Color figure can be viewed at wileyonlinelibrary.com]

clusters of grains in the PNZT seed on the Pt with smaller grain size (~25 nm) as shown in Figure 2A. In contrast, fewer defective areas were observed in the seed layer on the Pt with larger grain size (>200 nm) as shown in Figure 2B. In addition, it was found that the PNZT grain size of the seed layer increases with larger Pt grain size. The influence of Pt grain size on the PNZT grain size and surface pyrochlore coverage is similar to that reported in Borman et al's[12] work. This dependency is attributed to Pb loss through the bottom Pt electrode and PbO vaporization during processing.[17] As the Pb deficiency increases, the pyrochlore phase is favored (Pb-rich films favor the perovskite phase).[6,18] Figure 2B-E shows microstructures of MPB PNZT seed layers with increasing amounts of Pb excess in the solution. There are still some defective area with 20 at% Pb excess in the solution, as indicated by arrows in Figure 2C. As the amount of Pb excess in the solution increases, the area fraction of defective nucleation reduces, and it completely disappears above 25 at% Pb excess. It is also apparent that the grain size distribution becomes bi-modal as a function of Pb excess in the solution. However, the Lotgering factor for {100} orientation decreased above 25 at% Pb excess. Therefore, the optimal content of Pb excess in the solution for these bottom electrodes is about 20 at%.

Figure 2F shows the microstructure of a Ti-rich PNZT seed layer with 20 at% Pb excess. Unlike the MPB PNZT seed (Figure 2C), there is no defective area. However, a smaller grain size was observed, which may be related to a higher density of nucleation events for the Ti-rich composition. It is known that nucleation is the rate-limiting step for perovskite formation in sol-gel PZT films, and that $PbTiO_3$ has a lower activation energy for the perovskite formation than Zr-rich compositions.[14]

Figure 3A shows a cross-sectional SEM image of a PNZT seed layer which has a defective area between PNZT grains; high-resolution TEM (HRTEM) images of a defective area and PNZT grains in the seed layer are shown in Figures 3B-D. The defective area consists of an agglomeration of nanoparticles throughout the entire thickness. In contrast, the PNZT grain has clear lattice fringes, which demonstrates that the grain is well crystallized and oriented. The lattice spacings of the PNZT phase and Pt were obtained by performing a fast Fourier transform (FFT) on the HRTEM images in Figure 3C,D. The lattice spacings were compared to those obtained from the XRD pattern in Figure 1B. The lattice spacings of {111} plane of Pt from the XRD pattern and the HRTEM image were about 2.254 and 2.250 Å respectively, which are similar to the reported 2.265 Å from PDF# 89-7382. The small decrease of lattice spacing could be from tensile stress in the Pt after annealing.[19] The obtained out-of-plane d spacing of PNZT grain from TEM images was about 4.06 ± 0.03 Å. This is close to the one from the XRD pattern in Figure 1B (4.0264 ± 0.0004 Å).

STEM-EDS was performed on a PNZT grain and in a defective area; the resulting elemental analysis is summarized in Table 1. The signal from the Nb dopant was very weak due to the low doping level as well as the small sampling volume. As a result, Nb is not included in the table. It was found that the grain has a nearly stoichiometric composition. In contrast, the defective area is clearly Pb deficient compared to the grain composition. The concentrations of Zr and Ti in the defective area are higher than in the PNZT grain, but the Zr/Ti ratio is similar between the PNZT grain and the defective area.

Of interest is whether these defective areas significantly influence the properties or lifetime of devices made from thick PNZT layers on top of the seeds. To investigate this, 15 wt% PNZT-E1 solution with 16 at% Pb excess was used for bulk PNZT deposition on top of the seed layers discussed above. This 16 at% Pb excess in the solution was chosen because a higher Pb excess could decrease either the dielectric breakdown strength or the minimum electric field that induces cracking of the PZT film.[20] It should be pointed out that the degree of {100} orientation of the perovskite portion of the PNZT seed was independent of the amount of defective area (pyrochlore phase). In addition, bulk PNZT films on these seed layers had Lotgering factors >0.96, which should produce a large piezoelectric response. The remanent polarization of these films all exceeded 20 $\mu C/cm^2$, and the loops were well saturated and showed little leakage. The small signal dielectric permittivities were around 1500, and the loss tangents were

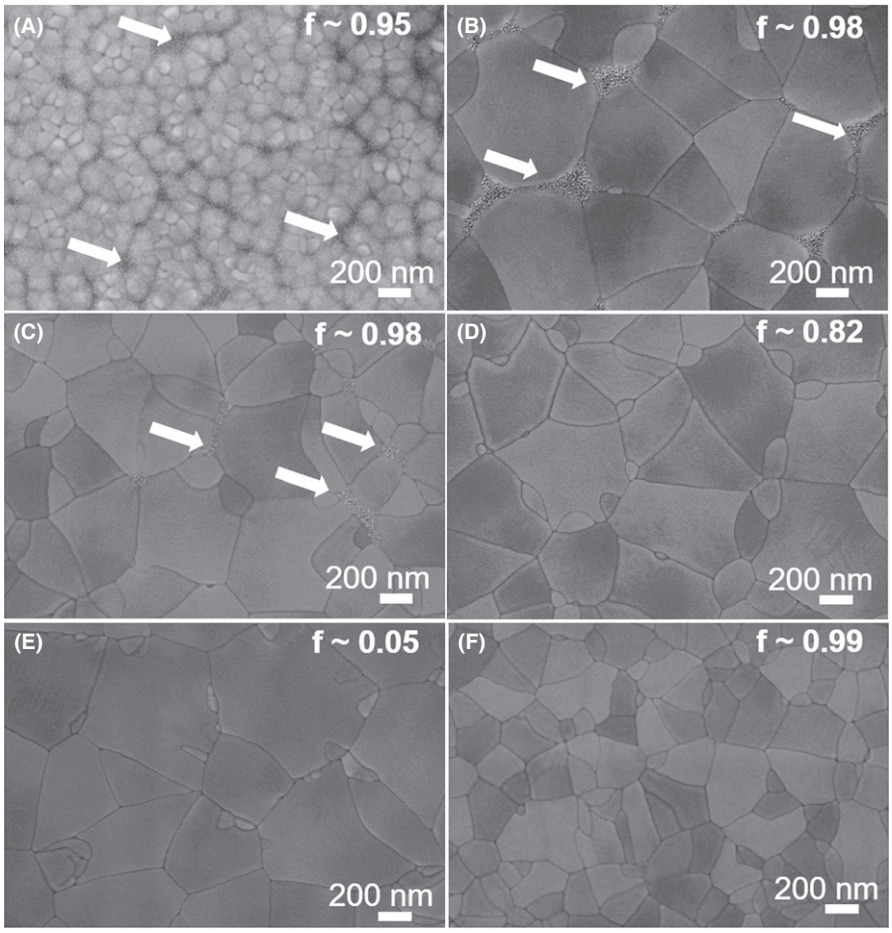

FIGURE 2 Scanning electron microscopy (SEM) images of Nb-doped PZT (PNZT) seed layers prepared from solutions with (A) 10 at% Pb excess with Pt deposited at room temperature, (B) 14 at % Pb excess, (C) 20 at% Pb excess, (D) 25 at% Pb excess, (E) 30 at% Pb excess, and (F) 20 at% Pb excess in the solution with Pt deposited at high temperature. A-E, is morphotropic phase boundary (MPB) composition and (F) is a Ti-rich composition (Zr:Ti = 44:56). The f values in the figures are Lotgering factor of {100} orientation. The arrows in (A-C) are examples of defective area

below 3%. Since all films have similar basic properties and inkjet printheads prepared using these films showed adequate displacement levels, we focus on the dielectric breakdown strength and reliability, which are important factors in industrial applications.

Figure 4 shows the dielectric breakdown strength of thick PNZT films made with different seed layers (and hence different area fractions of defective material in the seed layers). The data in Figure 4 were collected from the final actuator devices, in which the PNZT films were patterned by a dry-etching process. More than 30 actuator devices were measured for the dielectric breakdown strength. These experiments clearly show that the dielectric breakdown strength of the bulk PNZT film increases as the portion of defective area in the seed layer decreases. It is probable that the defective areas concentrate the local electric field so that the dielectric breakdown strength drops.[21] It was found that the surface pyrochlore defect in the seed layer propagated even to the top surface of the bulk PNZT film especially in cases where improper processing conditions were utilized (eg, nonuniform heating on the hot plate due to wafer curvature during pyrolysis, having the wrong PbO partial pressure in the RTA chamber, etc.). When this occurred, it produced nonuniformity in the properties across the PNZT wafer. Thus, the dielectric breakdown strength of about 1 MV/cm with zero defective areas in the seed was achieved. This value is comparable with the dielectric breakdown strength of a well-prepared sputtered[22] or sol-gel derived PZT film.[23]

The durability and lifetime of the PZT film are important for the industrial application of these devices. While previous research has focused on blanket films,[24] this paper explored micromachined devices. The values of lifetime in this study were taken from released devices (electrode area ~5×10^{-4} cm^2). The median lifetime (t_{50}), at which half of the 12 devices from a given wafer failed, was obtained under high temperature and electric field (200°C and 300 kV/cm). Failure was defined as the time at which the leakage current increased by 100 times with respect to the minimum current value.

As shown in Figure 4, the median lifetime increased as the portion of the defective area in the seed decreased. The result is similar to the dielectric breakdown strength finding. PNZT-1, which had defective regions covering approximately 40% of the seed layer area, showed a median lifetime of 0.2 hour. PNZT-4, which had no defective areas in the seed layer, showed a median lifetime of 13.1 hour under these aggressive testing conditions.

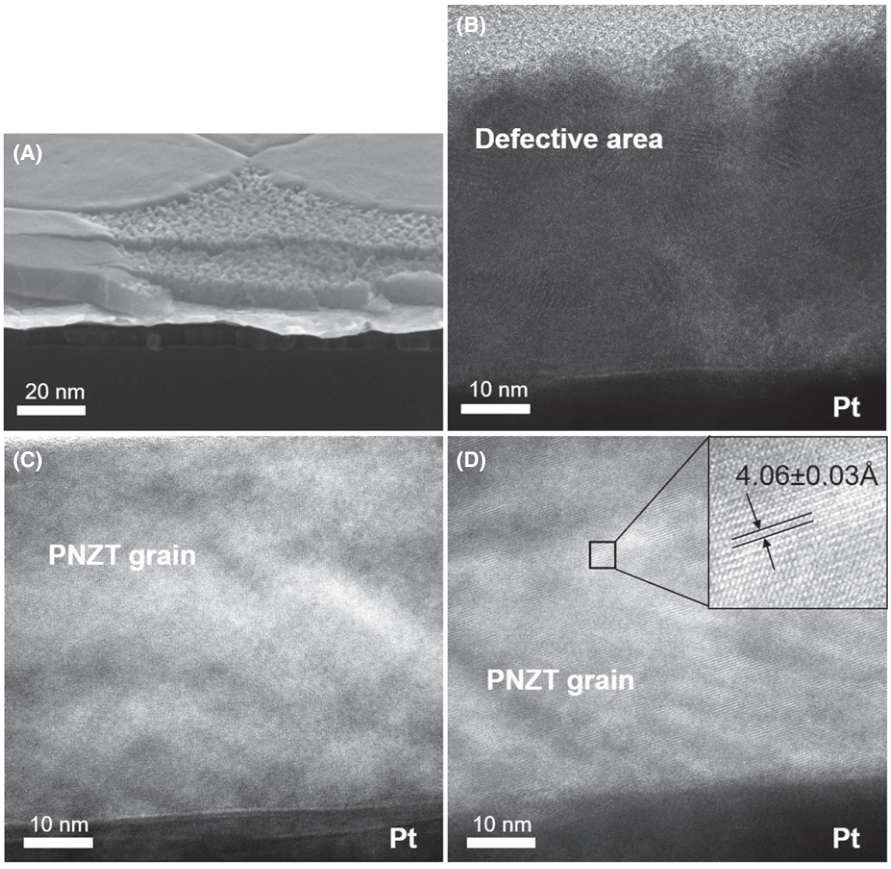

FIGURE 3 A, Scanning electron microscopy (SEM) image of cross section of Nb-doped PZT (PNZT) seed layer, (B) High-resolution TEM (HRTEM) image of defective area, (C) and (D) HRTEM images of PNZT grain in the seed layer (The insert shows a magnified image from which the out-of-plane D spacing was computed)

TABLE 1 Quantity of each element in the grain and defective area obtained by transmission electron microscopy-energy-dispersive spectrometry (TEM-EDS) analysis

Element (at%)	Grain	Defective area
Pb	24.8	17.2
Zr	16.0	17.9
Ti	11.9	13.7
O	47.4	51.3

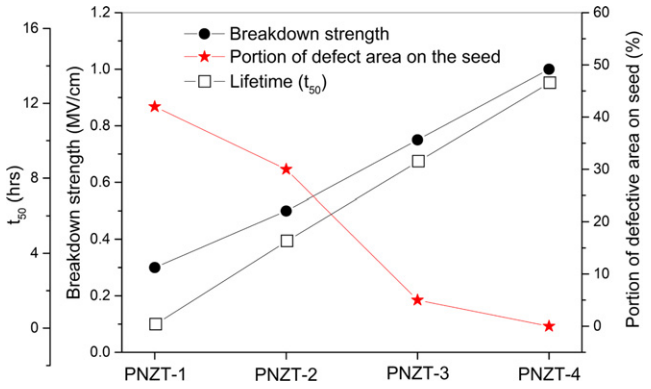

FIGURE 4 Dielectric breakdown strength and lifetime (t_{50}) of different Nb-doped PZT (PNZT) devices made from seed layers with different portion of defective area. 10, 14, and 20 at% Pb excess morphotropic phase boundary (MPB) compositions were used as seed layers for PNZT-1, PNZT-2, and PNZT-3 respectively. A 20 at% Pb excess Ti-rich composition was used as a seed layer for PNZT-4 [Color figure can be viewed at wileyonlinelibrary.com]

Additionally, the samples were measured under different HALT temperature and voltage conditions. For devices from a given PNZT-4 film, three tests were conducted at a constant voltage at different temperatures and three tests at a constant temperature with varied voltage. Figure 5A presents the median lifetime plotted as a function of the inverse of temperature. The median lifetimes under 300 kV/cm at 160, 180, and 200°C were determined to be 166.7, 41.8, and 13.1 hours, respectively. The measured activation energy for failure was 1.12 ± 0.03 eV. This value is similar to the previously reported activation energy for hole migration between V_{Pb}'' in thin film PZT.[16,25,26] Figure 5B shows the dependence of the median lifetime on voltage. The median lifetimes under 200°C at 200, 250, and 300 kV/cm were determined to be 73.0, 27.7, and 13.1 hours, respectively. The voltage acceleration factor is around 4.24 ± 0.07, which is also close to previous reports.[26,27]

Both the activation energy for failure and the voltage acceleration factor were found to depend on the quality of the seed layer. The activation energy decreased to 0.51 ± 0.08 eV for the PNZT-1 film which contained the

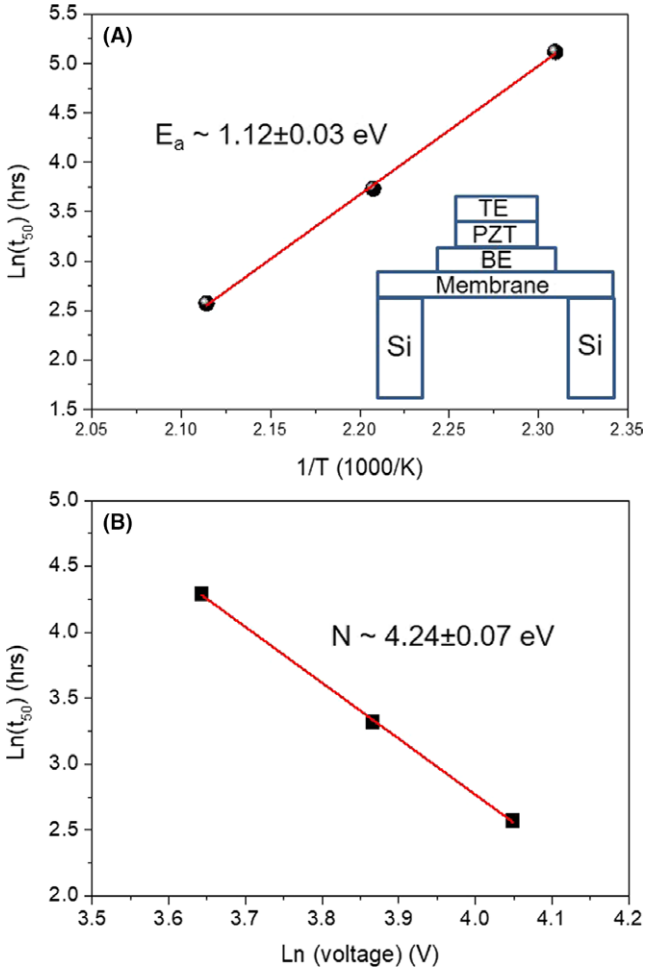

FIGURE 5 A, Highly accelerated lifetime testing (HALT) data at a constant voltage for different temperatures and (B) HALT data at a constant temperature at different voltages of Nb-doped PZT (PNZT)-4 film. The inset is a simplified schematic of the cross section of the actual device (BE, bottom electrode, TE, top electrode) [Color figure can be viewed at wileyonlinelibrary.com]

largest defective area fraction in the seed layer. The lower activation energy clearly corresponds to a different failure process. Two possibilities that might account for the lower activation energy would be oxygen vacancy migration[28] or a decrease in the Schottky barrier height with the electrodes. Further investigation is required to identify the failure mechanisms. In addition, the voltage acceleration factor increased for films with a larger area fraction of defective region in the seed layer to 6.28 ± 0.08. Thus, film grown from defective seed layers are more voltage sensitive.

4 | CONCLUSIONS

A well-oriented PNZT seed layer without defective areas was developed. It was confirmed that the degree of {100} orientation was independent of the proportion of defective area in the seed layer; in contrast the dielectric breakdown strength and reliability of devices prepared from these films strongly depended on the amount of defective area in the seed layer. The defective area consisted of nanoparticles and had a Pb-deficient composition. The lifetime and dielectric breakdown strength of PNZT film-based actuators were improved as the proportion of defective area in the seed layer decreased. The activation energy and voltage acceleration factor for failure of devices were 1.12 ± 0.03 eV and 4.24 ± 0.07 respectively.

ORCID

Song Won Ko http://orcid.org/0000-0002-3238-389X
Trent Borman http://orcid.org/0000-0003-4916-9678
Susan Trolier-McKinstry http://orcid.org/0000-0002-7267-9281

REFERENCES

1. Muralt P, Polcawich RG, Trolier-McKinstry S. Piezoelectric thin films for sensors, actuators, and energy harvesting. MRS Bull. 2009;34:658–64.
2. Muralt P. Recent progress in materials issues for piezoelectric MEMS. J Am Ceram Soc. 2008;91:1385–96.
3. Trolier-McKinstry S, Muralt P. Thin film piezoelectrics for MEMS. J Electroceram. 2004;12:7–17.
4. Baek SH, Park J, Kim DM, Aksyuk V, Das RR, Bu SD, et al. Giant piezoelectricity on Si for hyperactive MEMS. Science. 2011;334:958–61.
5. Hiboux S, Muralt P. Mixed titania-lead oxide seed layers for PZT growth on Pt(111): a study on nucleation, texture and properties. J Eur Ceram Soc. 2004;24:1593–6.
6. Keech R, Shetty S, Kuroda MA, Liu XH, Martyna GJ, Newns DM, et al. Lateral scaling of $Pb(Mg_{1/3}Nb_{2/3})O_3$-$PbTiO_3$ thin films for piezoelectric logic applications. J Appl Phys. 2014;115:234106.
7. Yeo HG, Ma X, Rahn C, Trolier-McKinstry S. Efficient piezoelectric energy harvesters utilizing (001) textured bimorph PZT films on flexible metal foils. Adv Funct Mater. 2016;26:5940–6.
8. Gong W, Li JF, Chu X, Gui Z, Li L. Preparation and characterization of sol-gel derived (100)-textured Pb(Zr, Ti)O_3 thin films: PbO seeding role in the formation of preferential orientation. Acta Mater. 2004;52:2787–93.
9. Jaffe B, Roth RS, Marzullo S. Piezoelectric properties of lead zirconate-lead titanate solid-solution ceramics. J Appl Phys. 1954;25:809–10.
10. Aggarwal S, Madhuka S, Nagaraj B, Jenkins IG, Ramesh R, Boyer L, et al. Can lead nonstoichiometry influence ferroelectric properties of Pb(Zr, Ti)O_3 thin films? Appl Phys Lett. 1999;75:716–8.
11. Yeo HG, Trolier-Mckinstry S. 001 Oriented piezoelectric films prepared by chemical solution deposition on Ni foils. J Appl Phys. 2014;116:14105.
12. Borman T, Ko SW, Mardilovich P, Trolier-McKinstry S. Development of crystallographic texture in chemical solution deposited

lead zirconate titanate seed layers. J Am Ceram Soc. 2017;100:4476–82.
13. Zhu W, Fujii I, Ren W, Trolier-McKinstry S. Domain wall motion in A and B site donor-doped $Pb(Zr_{0.52}Ti_{0.48})O_3$ films. J Am Ceram Soc. 2012;95:2906–13.
14. Kwok CK, Desu SB. Low temperature perovskite formation of lead zirconate titanate thin films by a seeding process. J Mater Res. 1993;8:339–44.
15. Prokopowicz T, Vaskas A. Final report, ECOM-9705-F, 1969 NTIS AD-864068.
16. Garten LM, Hagiwara M, Ko SW, Trolier-McKinstry S. Physically based DC lifetime model for lead zirconate titanate films. Appl Phys Lett. 2017;111:122903.
17. Lefevre MJ, Speck JS, Schwartz RW, Dimos D, Lockwood SJ. Microstructural development in sol-gel derived lead zirconate titanate thin films: the role of precursor stoichiometry and processing environment. J Mater Res. 1996;11:2076–84.
18. Bastani Y, Bassiri-Gharb N. Processing optimization of lead magnesium niobate-lead titanate thin films for piezoelectric MEMS application. J Am Ceram Soc. 2012;95:1269–75.
19. Corkovic S, Whatmore RW, Zhang Q. Development of residual stress in sol-gel derived $Pb(Zr, Ti)O_3$ films: an experimental study. J Appl Phys. 2008;103:084101.
20. Borman TM, Zhu W, Wang K, Ko SW, Mardilovich P, Trolier-McKinstry S. Effect of lead content on the performance of niobium-doped 100 textured lead zirconate titanate films. J Am Ceram Soc. 2017;100:3558–67.
21. Levi RD, Samantaray MM, Trolier-McKinstry S, Randall CA. Influence of substrate microstructure on the high field dielectric properties of $BaTiO_3$ films. J Appl Phys. 2008;104:104117.
22. Hishinuma Y, Fujii T, Naono T, Arakawa T, Li Y. Recent progress on development of sputtered PZT film at FUJIFILM. Proceedings of the IEEE International Symposium on Applications of Ferroelectrics. 2015; 288–91.
23. Udayakumar KR, Schuele PJ, Chen J, Krupanidhi SB, Cross LE. Thickness-dependent electrical characteristics of lead zirconate titanate thin films. J Appl Phys. 1995;77:3981–6.
24. Polcawich RG, Feng CN, Kurtz S, Perini S, Moses PJ, Trolier-McKinstry S. AC and DC electrical stress reliability of piezoelectric lead zirconate titanate (PZT) thin films. Int J Microcircuits Electron Packag. 2000;23:85–91.
25. Al-Shareef HN, Dimos D. Leakage and reliability characteristics of lead zirconate titante thin-film capacitors. J Am Ceram Soc. 1997;80:3127–32.
26. Polcawich RG, Feng C, Vanatta P, Piekarz R, Trolier-McKinstry S, Dubey M, et al. Highly accelerated lifetime testing (HALT) of lead zirconate titanate (PZT) thin films. Proc 12th IEEE Inter Symp Appl Ferro. 2000;1:357–60.
27. Al-Shareef H, Dimos D, Dimes D. Accelerated life-time testing and resistance degradation of thin-film decoupling capacitors. Proc Tenth IEEE Int Symp Appl Ferroelectr. 1996;1:421–5.
28. Randall CA, Maier R, Qu W, Kobayashi K, Morita K, Mizuno Y, et al. Improved reliability predictions in high permittivity dielectric oxide capacitors under high dc electric fields with oxygen vacancy induced electromigration. J Appl Phys. 2013;113:014101.

SUPPORTING INFORMATION

Additional supporting information may be found online in the Supporting Information section at the end of the article.

How to cite this article: Ko SW, Zhu W, Fragkiadakis C, et al. Improvement of reliability and dielectric breakdown strength of Nb-doped lead zirconate titanate films via microstructure control of seed. *J Am Ceram Soc*. 2019;102:1211–1217. https://doi.org/10.1111/jace.15940